

Ada-NAV: Adaptive Trajectory Length-Based Sample Efficient Policy Learning for Robotic Navigation

Bhrij Patel¹, Kasun Weerakoon¹, Wesley A. Suttle², Alec Koppel³,
Brian M. Sadler⁴, Tianyi Zhou¹, Amrit Singh Bedi⁵, and Dinesh Manocha¹

Abstract— Trajectory length stands as a crucial hyperparameter within reinforcement learning (RL) algorithms, significantly contributing to the sample inefficiency in robotics applications. Motivated by the pivotal role trajectory length plays in the training process, we introduce Ada-NAV, a novel adaptive trajectory length scheme designed to enhance the training sample efficiency of RL algorithms in robotic navigation tasks. Unlike traditional approaches that treat trajectory length as a fixed hyperparameter, we propose to dynamically adjust it based on the entropy of the underlying navigation policy. Interestingly, Ada-NAV can be applied to both existing on-policy and off-policy RL methods, which we demonstrate by empirically validating its efficacy on three popular RL methods: REINFORCE, Proximal Policy Optimization (PPO), and Soft Actor-Critic (SAC). We demonstrate through simulated and real-world robotic experiments that Ada-NAV outperforms conventional methods that employ constant or randomly sampled trajectory lengths. Specifically, for a fixed sample budget, Ada-NAV achieves an 18% increase in navigation success rate, a 20–38% reduction in navigation path length, and a 9.32% decrease in elevation costs. Furthermore, we showcase the versatility of Ada-NAV by integrating it with the Clearpath Husky robot, illustrating its applicability in complex outdoor environments.

I. INTRODUCTION

Autonomous robotic navigation is ubiquitous in tasks such as search-and-rescue [1], disaster relief [2], and planetary exploration applications [3]. While traditional navigation methods have been popular among the community [4]–[6], reinforcement learning (RL) [7] has been recently successful in robotic navigation tasks [8]. RL-based methods offer advantages in terms of being mapless, having lower dependence on the sensor accuracy, and possessing the ability to work with raw sensor data [8]–[10]. However, the benefits of RL come with their own set of intricate challenges, most prominently the issue of exploration in the environment during training. Traditional RL methods often hinge on the availability of a dense reward structure [11], which may rarely be available in complex, unpredictable environments [12]–[15]. These challenges make the existing RL methods

¹Department of Computer Science, University of Maryland, College Park, MD, USA. Emails: {bbp13, kasunw, tianyi, dmanocha}@umd.edu

²U.S. Army Research Laboratory, Adelphi, MD, USA. Email: wesley.a.suttle.ctr@army.mil

³JP Morgan AI Research, New York, NY, USA. Email: alec.koppel@jpmchase.com

⁴University of Texas at Austin, Austin, TX, USA. Email: brian.sadler@ieee.org

⁵Department of Computer Science, University of Central Florida, Orlando, FL, USA. Email: amritsingh.bedi@ucf.edu

This work was supported by Army Cooperative Agreement W911NF2120076. We acknowledge the support of the Maryland Robotics Center and Northrup Grumman Seed Grant 2022.

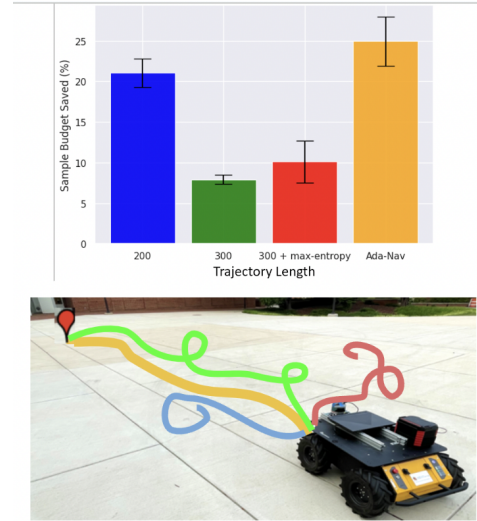


Fig. 1: Robot navigation using policies trained with the REINFORCE policy gradient algorithm using four trajectory length schemes. We compare three fixed trajectory lengths, 200 (blue), 300 (green), and 300 with max entropy regularization (red), against Ada-NAV (ours) (yellow) in real-world environments. More details can be found in Sec. IV. The drawn trajectories are sample representations of the robot’s odometry data collected during each navigation task. Ada-NAV enhances sample efficiency of training (shown in the figure by the lower value of the orange bar plot) by adaptively varying trajectory length throughout training. Ada-NAV results in better navigation policies compared to baseline approaches and generates shorter and more successful test-time trajectories.

sample inefficient during training, especially for robotics applications where rewards are sparse [16], [17], since the agent does not receive constant feedback on its progression towards the goal.

To improve the sample efficiency of RL for robotics navigation, common existing methods include reward-shaping [18] and learning from demonstrations [19], [20]. Reward-shaping methods use pseudo-rewards to encourage exploration in the environment [11], [21]. However, these methods require an expert to design intrinsic rewards, which can lead to performance-hindering bias. Furthermore, collecting expert-guided demonstrations for navigation tasks can be challenging and expensive to obtain [22].

In this work, we present Ada-NAV, a general technique for improving the sample efficiency of RL methods for robotics navigation tasks with minimal modifications to the existing state-of-the-art methods in the literature. Our key idea is to focus on adaptively changing a salient feature in most RL methods: trajectory length. We note that in policy gradient

algorithms, trajectory length is the number of interactions the robot has with the environment before each gradient update during training. For navigation, an interaction is any action the mobile robot takes and the resulting state in the environment and the reward it receives. It has been verified in the literature that short trajectory lengths can lead to inefficient learning, while long ones can be unreliable when in an unfamiliar environment [23]. Ada-NAV resolves this issue by having an adaptive trajectory length which is reliable and computationally tractable.

In this work, we utilize a previously unexplored connection between a policy's mixing time and its policy entropy to formulate Ada-NAV. To develop Ada-NAV, our novel approach is to start by connecting the trajectory length to the *mixing time* of the policy that generates the trajectory. The mixing time of a policy is the amount of time it takes for a robot to reach its limiting behavior under that policy. When mixing time is large, ensuring that trajectories are sufficiently long is important for obtaining accurate estimates of system behavior and algorithmic essentials, such as policy gradients [24]. When mixing time is short, on the other hand, ensuring trajectory lengths are commensurate frees up effort for performing more rapid policy updates and environmental exploration. Unfortunately, mixing time is typically difficult to estimate in complex environments [25], [26], so proxy methods for determining trajectory length are needed.

Main Contributions: Ada-NAV increases sample efficiency by controlling the amount of data required to update the policy parameter, thus decreasing the number of training samples needed to learn an optimal policy for robot navigation tasks. Our specific contributions include:

- We empirically establish a positive correlation between the policy entropy and the spectral gap of its induced Markov chain. We show that this correlation is present with various transition dynamics. This insight motivates our use of the changing policy entropy as a dynamic variable to control trajectory length.
- We take advantage of this empirical insight by utilizing a monotonic mapping between policy entropy and trajectory length to facilitate exploration in environments with sparse rewards and serve as the foundation for our adaptive trajectory length scheme, Ada-NAV.
- We present extensive empirical results using multiple RL methods, including REINFORCE [27] and Proximal Policy Optimization (PPO) [28] and Soft Actor-Critic (SAC) [29], to show that Ada-NAV improves the sample efficiency with both on-policy and off-policy methods. Our experiments in goal-reaching navigation tasks with both even and uneven terrains demonstrate that Ada-NAV outperforms constant trajectory length schemes, even those utilizing maximum entropy regularization, in terms of sample efficiency.
- We evaluate the navigation performance of Ada-NAV in both simulated and real-world outdoor environments using a Clearpath Husky robot. We observe that, for a fixed sample budget, Ada-NAV leads to an 18% increase in navigation success rate, a 20-38% decrease in the navigation path length, and a 9.32% decrease in the elevation cost compared to the policies obtained by the

other methods.

A. Related Works

In this section we give a brief overview of the existing work related to RL for autonomous navigation and sparse rewards.

RL for Navigation: Motion planning and navigation has been well studied in robotics [4]–[6]. RL-based methods have been extensively used for robot navigations [30]. Methods such as DDPG [31], A3C [32], and DQN [33] have been used for outdoor navigation, while [34] learned a global map to find the shortest path out of a maze with RL. [35] used classical methods to create a hierarchical RL approach. For policy gradient methods, [36] demonstrated the superior performance of Soft Actor-Critic (SAC) over deep deterministic policy gradient (DDPG) in the navigation of mobile robots. In these policy gradient methods, it is well known that the gradient estimation requires lots of samples and the overall training procedure is sample inefficient.

Sparse Rewards: For model-free reinforcement learning, reward sparsity greatly affects policy search [11], [37] as a mobile robot will rarely receive any feedback to adjust its behavior. To produce more rewards which the algorithm can learn from, reward-shaping methods based on intrinsic rewards have been proposed. Methods in [38] and [21] modified the reward output to encourage exploration of the environment. [39] and [40] used imitation learning and demonstrations to overcome the challenges of sparse rewards. Curriculum learning has also been utilized to deal with sparse rewards in navigation. [41] divided the navigation task into a subgoal tree so the agent can learn from dense-to-sparse curriculum. [17] and [42] formulated a heavy-tailed policy to encourage exploration in sparse environments.

II. PROBLEM FORMULATION

A. Reinforcement Learning and Policy Gradient Methods

We consider a Markov Decision Process (MDP) characterized by the tuple $\mathcal{M} := (\mathcal{S}, \mathcal{A}, \mathbb{P}, r)$, where \mathcal{S} is the state space for the robot in the environment, \mathcal{A} is the set of possible actions the robot can take, \mathbb{P} is the transition probability kernel that determines the next state $s' \in \mathcal{S}$ given $s \in \mathcal{S}, a \in \mathcal{A}$ via $s' \sim \mathbb{P}(\cdot|s, a)$, and $r : \mathcal{S} \times \mathcal{A} \rightarrow [0, r_{\max}]$ is the reward function. The mobile robot navigates through this environment using a (potentially stochastic) policy π that provides a conditional probability distribution over actions a given a state s . Given a policy π and transition kernel \mathbb{P} , the transition dynamics of the Markov chain induced by π over \mathcal{M} is given by $\mathbb{P}_\pi(s'|s) = \sum_{a \in \mathcal{A}} \mathbb{P}(s'|s, a)\pi(a|s)$. The goal in the RL setting is to find a policy maximizing long-run reward over \mathcal{M} . To achieve this, one infinite-horizon objective typically considered in the RL literature is expected discounted reward given by

$$J^\gamma(\pi) = \mathbb{E}_{\pi, \mu} \left[\sum_{t=0}^{\infty} \gamma^t r(s_t, a_t) \right], \quad (1)$$

where $\gamma \in (0, 1)$ is some pre-specified discount factor and μ is a given initial start state distribution over \mathcal{S} . In (1), the expectation is over the policy and initial state distributions. In the discounted-reward settings, the state-action value

function corresponding to a given policy π is defined by $Q_\pi^\gamma(s, a) = \mathbb{E}_\pi [\sum_{t=0}^{\infty} \gamma^t r(s_t, a_t) \mid s_0 = s, a_0 = a]$.

Policy Gradient Algorithm. To handle large, potentially continuous state and action spaces, we focus on the case where policy π is parameterized by a vector $\theta \in \mathbb{R}^d$, where d denotes the parameter dimension, leading to the notion of a parameterized policy π_θ . We define $J^\gamma(\theta) = J^\gamma(\pi_\theta)$. Then, following policy gradient theorem [43], we note that

$$\nabla J^\gamma(\theta) = \mathbb{E}_{\pi_\theta, \mu} [Q_\pi^\gamma(s, a) \nabla \log \pi_\theta(a|s)], \quad (2)$$

which provides the gradient expression to perform gradient ascent on the objectives $J^\gamma(\theta)$. For the discounted setting, at time t the policy gradient estimate is obtained by generating a $K \in \mathbb{N}$ length trajectory $\tau_t := \{s_t, a_t, \dots, s_{t+K-1}, a_{t+K-1}\}$ using π_{θ_t} , and then computing

$$\widehat{\nabla J^\gamma(\theta_t)} = \sum_{k=0}^{K-1} \gamma^k r(s_{t+k}, a_{t+k}) \nabla \log \pi_{\theta_t}(a_t|s_t). \quad (3)$$

This expression is then used to perform a gradient update of the form $\theta_{t+1} = \theta_t + \alpha \widehat{\nabla J^\gamma(\theta_t)}$, for some stepsize $\alpha > 0$. In REINFORCE, increasing K naturally improves the quality of the estimator given in Equation (3) [44], but at the cost of an increased number of samples. In reinforcement learning for robotic navigation, simulation data to train mobile agent can be expensive to obtain or generate. Thus, reducing the number of training sample needed without degrading navigation performance is crucial in mitigating operation costs. In the next section, we will explain the quantity mixing time and its importance to trajectory length selection.

B. Mixing Time and Spectral Gap

In policy gradient algorithms an important issue is that, to obtain good estimates of the expectation (2), which is taken with respect to the stationary distribution induced over the underlying MDP by π_θ , longer trajectories are often needed. The length of the trajectories is dictated by the mixing time – to be defined below – of the associated policy. Recent work on stochastic optimization [45] and policy gradient (PG) methods [24] has highlighted and clarified the connection between Markov chain mixing time and ideal trajectory length. To leverage this connection in our approach, we first present some relevant terminology and results.

We assume throughout that, for a given policy parameter θ , the Markov chain induced by π_θ on the MDP \mathcal{M} is irreducible and aperiodic, which is a common assumption in theoretical analyses of RL methods. First note that the ergodicity assumption guarantees that the Markov chain has a unique stationary distribution μ_θ . For an MDP $\mathcal{M} = (\mathcal{S}, \mathcal{A}, \mathbb{P}, r)$ and policy π_θ , the ϵ -mixing time of π_θ is $\tau_{mix}^\theta(\epsilon) := \inf\{t : \sup_{s \in \mathcal{S}} \|\mathbb{P}_{\pi_\theta}^t(\cdot|s) - \mu_\theta(\cdot)\|_{TV} \leq \epsilon\}$. By convention, the mixing time is defined as $\tau_{mix}^\theta := \tau_{mix}^\theta(1/4)$.

Though mixing times are useful in determining appropriate trajectory lengths, they are typically difficult to estimate in practice. Therefore, an alternative to estimating mixing time is estimating a lower bound. One such quantity that has been established to lower bound mixing time is the absolute spectral gap, or simply spectral gap, of the induced transition matrix \mathbb{P}_{π_θ} , defined to be the difference between 1 and the second largest eigenvalue, λ_θ^* . As demonstrated in [46], the

spectral gap and mixing time of a Markov chain bear the following relationship.

Theorem 2.1: Let $\lambda_\theta \neq 1$ be an eigenvalue of the transition matrix \mathbb{P}_{π_θ} . Then

$$\tau_{mix}^\theta(\epsilon) \geq \left(\frac{1}{1 - |\lambda_\theta|} - 1 \right) \log \left(\frac{1}{2\epsilon} \right). \quad (4)$$

Taking $\epsilon = 1/4$ and noticing that λ_θ^* gives the tightest lower bound, we have $\tau_{mix}^\theta \geq (1/(1 - |\lambda_\theta^*|) - 1) \log 2$. When an estimate of \mathbb{P}_{π_θ} is available, this provides a method for bounding its mixing time τ_{mix}^θ . Unfortunately, estimating \mathbb{P}_{π_θ} is not always practical in large and complex state and action spaces [25], [26]. Thus, a proxy for the spectral gap is crucial for navigation in complex environments. In the following section, we leverage this theorem to empirically establish a useful connection between policy entropy and spectral gap to adaptively change trajectory length with no need to estimate \mathbb{P}_{π_θ} .

III. PROPOSED APPROACH: ADAPTIVE TRAJECTORY-BASED POLICY LEARNING

Before presenting our main algorithm, Ada-NAV, we start by highlighting an interesting connection between a policy entropy and the spectral gap of its induced transition matrix.

A. Key Insight: Policy Entropy as a Proxy for Mixing Time

Given a policy π_θ , we would ideally like to base trajectory length for our PG updates on the spectral gap from the mixing time lower bound in Theorem 4. However, without prior knowledge of the transition kernel \mathbb{P} of the underlying MDP, it is difficult to calculate the spectral gap of the induced transition matrix, \mathbb{P}_{π_θ} . One possible workaround is to estimate the transition kernel, but this quickly becomes intractable due to the $\Omega(|\mathcal{S}||\mathcal{A}|)$ number of samples required for each estimate. Interestingly, one key insight we observe is that if the policy becomes more deterministic and thus the entropy decreases, the spectral gap of the induced transition matrix also decreases or stays the same, suggesting a monotonic relationship between mixing time and policy determinism.

Figure 2 illustrates this correlation with a 2D gridworld environment. We have a 25-by-25 gridworld. Each plot in Figure 2 corresponds to a different fixed transition probability kernel \mathbb{P} . For each fixed kernel, we construct 100 tabular policies, each with a discrete action space of 5 elements to represent up, down, left, right, and stay. The tabular policies have various average entropies, ranging from maximum entropy with uniform probability over the action space for each state (end of x-axis on Figure 2) to completely deterministic for each state (beginning of x-axis) with a probability of 1 of moving upwards. We define policy entropy in for tabular policies as the average Shannon entropy across all states, see Equation 5. For each policy, we multiply the policy with the fixed transition kernel to calculate the underlying Markov Chain and then estimate its spectral gap.

In this environment, if the agent chooses an action that would make it go off the edge, the agent will stay in the current state. Both transition kernels are deterministic: each state-action pair is mapped to a single next state a potential agent can occupy. One kernel represents an empty gridworld

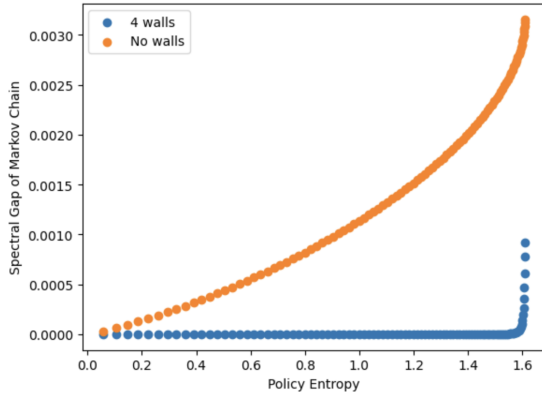


Fig. 2: Positive correlation between a policy’s entropy and the spectral gap of its induced transition matrix over a 25-by-25 gridworld environment with different fixed transition kernels. Policy entropy is a viable proxy for mixing time.

with no obstacles. The relationship between spectral gap and policy entropy is plotted in orange for this kernel. The other kernel is represents a gridworld with 4 walls dividing it into 4 equal regions. Please see Appendix for visualization. The plot corresponding to this kernel is blue in Figure 2.¹

To be clear, in these experiments, we have not trained any agent to navigate in the gridworld. We have a static environment where we manually designed transition kernel matrices and multiplied each one with 100 different tabular policies to estimate the underlying Markov Chains and their corresponding spectral gaps, a task normally intractable for more complex, realistic environments. For results displaying Ada-NAV’s effectiveness in increasing sample efficiency for a goal-reaching task in this environment and other gridworld environments, please see the Appendix.

As previously mentioned, we define the policy entropy in the discrete action space case as average the Shannon entropy [47] over the state space:

$$H(\pi_\theta) = -\frac{1}{|\mathcal{S}|} \sum_{s \in \mathcal{S}} \sum_{a \in \mathcal{A}} \pi_\theta(a|s) \log \pi_\theta(a|s). \quad (5)$$

In the continuous action space case for the robotic navigation experiments in Section IV, we use the closed-form differential entropy for a multivariate Gaussian distribution,

$$H(\pi_\theta) = -\frac{1}{|\mathcal{S}|} \sum_{s \in \mathcal{S}} \frac{1}{2} \log((2\pi e)^N \det(\Sigma_\theta(s))). \quad (6)$$

where N is the action space dimension and $\Sigma_\theta(s)$ is the covariance matrix of the policy $\pi_\theta(\cdot|s)$. We note that there are no analytical equations to calculate mixing time, and calculating spectral gap requires knowledge of the transition dynamics $P(s'|s, a)$ which restricts it to only model-based RL. Thus, using analytical Equations (5) and (6) as a proxy for mixing time is a more simple method that can be used for either model-free or model-based RL.

B. Ada-NAV: Mapping Policy Entropy to Trajectory Length

We now present our novel adaptive trajectory length scheme for robotic navigation. The key to our approach is to

¹Code to notebook to generate plot: https://github.com/bridge00/spectral_gap_policy_entropy.git

Algorithm 1 Policy Learning with Ada-NAV

```

1: Initialize: policy parameter  $\theta_0$ , policy entropy  $H_i$ , trajectory length  $t_i$ , current trajectory length  $t_c = t_i$ , maximum trajectory length  $t_d$ , number of episodes  $E$ , maximum number  $K$  of iterations per episode, sensitivity parameter  $\eta$ ,  $t = 0$ 
2: for  $e = 0, \dots, E - 1$  do
3:   calculate  $H_c$  using 5 for discrete actions, 6 for continuous actions
4:   calculate  $t_c$  using 7
5:    $k = 0$ 
6:   while  $k < K$  do
7:     collect trajectory
8:      $\mathcal{T} = (s_1, a_1, r_1), \dots, (s_{t_c}, a_{t_c}, r_{t_c})$  using  $\pi_{\theta_t}$ 
9:     Perform gradient update using  $\mathcal{T}$  to obtain  $\theta_{t+1}$ 
10:     $k = k + t_c$ 
11:     $t = t + 1$ 
12:   end while
13: end for
14: Return:  $\pi_{\theta_t}$ 

```

select trajectory length based on the current policy entropy value. We perform this computation using a monotonic mapping from the range of possible policy entropy values to a range of possible trajectory length values. Let H_i denote the maximum possible policy entropy value and H_c the policy entropy of the current policy. In practice, we choose $H_i = H(\pi_{\theta_0})$ to be the entropy of the initial policy, since policy entropy tends to decrease during training. Let $t_i \in \mathbb{N}$ denote the user-specified initial trajectory lengths and let $\eta > 0$ denote a user-specified sensitivity parameter that controls the rate of change of length (see the Appendix for specific values of t_i, η used). For our experiments, we determine the trajectory length corresponding to the current policy entropy using the mapping f below:

$$t_c = f_{t_i, \eta}^{H_i}(H_c) = \text{round} \left(1 - \frac{H_c}{H_i} \left(1 - \frac{t_i}{\eta} \right) \right), \quad (7)$$

where the rounding operation is to ensure that t_c is always an integer. In the Appendix, we utilize other monotonic transformation to map entropy to trajectory length in the form of an exponential function. Furthermore, in our experiments, we initialize our policies with a Gaussian distribution. To ensure, that H_c never increases too much so that t_c becomes 0, one can initialize with a uniform distribution so that H_i is the maximum possible entropy. Algorithm 1 summarizes our Ada-NAV methodology for adaptive trajectory length PG methods. Note that any on-policy PG method can be used to carry out the policy gradient update in line 3. The training is divided into episodes where the start location and goal are constant between episodes. During each episode, a gradient update occurs after every trajectory. The amount of samples in each trajectory is the trajectory length. The episode ends when goal is reached or when a set number of interactions have occurred. For clarification, given an episode, the trajectory length is fixed. At the start of the new episode is when the trajectory length is adjusted based on policy entropy.

IV. EXPERIMENTS AND RESULTS

This section provides a detailed empirical study and comparison of the proposed adaptive trajectory methods in Algorithm 1.



Fig. 3: Comparison of four different trajectory-length schemes on [LEFT] even and [RIGHT] uneven terrain navigation tasks in Unity-based outdoor robot simulator. For REINFORCE, PPO, and SAC, using Ada-NAV as the trajectory length scheme leads to a navigation policy with a higher cumulative reward return than using constant trajectory lengths. The drawn trajectories are sample representations of the robot’s odometry data collected during each navigation task. The trajectories pictured are representative of all three algorithms, since we found that each trajectory-length scheme leads to similar navigation behavior regardless of which RL algorithm is used. See Figures 4 and 6 for training details.

RL Algorithms. We choose three RL algorithms to integrate Ada-NAV into for improved sample efficiency: REINFORCE, PPO, and SAC. As REINFORCE and PPO are both on-policy policy gradient methods and SAC is an off-policy method, we show that Ada-NAV can improve the sample efficiency of various classes of policy gradient algorithms.

Baselines. Since our proposed approach relies on adaptive trajectory length, for each algorithm we test Ada-NAV with, we compare it against the same algorithm with fixed trajectory lengths. We also compare with fixed trajectory lengths with max-entropy regularizer as that also encourages exploration.

We also incorporate a classical navigation algorithm Ego-graph [48], to highlight the navigation performance of our method under challenging terrain conditions. Ego-graph is a baseline method in [48] that utilizes robot-centric elevation data to obtain the actions that minimize the elevation gradient cost.

Environments: We utilize two environments in a unity-based outdoor robot simulator. The policies for the outdoor robot simulator are based on the REINFORCE algorithm [27]. Finally, we deploy navigation policies trained for a fixed sample budget using the robot simulator on a real Clearpath Husky robot. We present the details of the training environments below:

Even and Uneven Terrain Navigation in Robotic Simulations: We use a Unity-based outdoor simulator with a Clearpath Husky robot model to train policies for two navigation tasks: 1. Goal Reaching, 2. Uneven terrain navigation using the Reinforce algorithms. The Unity simulator includes diverse terrains and elevations for training and testing. We restrict ourselves to a $100m \times 100m$ region during training. We used identical policy distribution parameters and neural

network architectures with all four algorithms during training and evaluation. The policies are implemented using Pytorch in to train in the simulator equipped with a Clearpath Husky robot model, and a ROS Melodic platform. The training and simulations are executed on a workstation with an Intel Xeon 3.6 GHz CPU and an Nvidia Titan GPU.

Our agent is a differential drive robot with a two-dimensional continuous action space $a = (v, \omega)$ (i.e. linear and angular velocities). The state space varies for the two navigation tasks and is obtained in real time from the simulated robot’s odometry and IMU sensors. The state inputs used in the two scenarios are, The simulator includes even and uneven outdoor terrains and a differential drive robot model with a two-dimensional continuous action space $a = (v, \omega)$ (i.e. linear and angular velocities). We perform two navigation tasks: 1. Even terrain, 2. Uneven terrain navigation using the robot’s local sensor data as state observations. The state space varies for the two navigation tasks and is obtained in real-time from the simulated robot’s odometry and IMU sensors. The state inputs used in the two scenarios are,

- $d_{goal} \in [0, 1]$ - Normalized distance (w.r.t the initial straight-line distance) between the robot and its goal;
- $\alpha_{goal} \in [0, \pi]$ - Angle between the robot’s heading direction and the goal;
- $(\phi, \theta) \in [0, \pi]$ - Roll and pitch angle of the robot respectively.

Inspired by [17], we define three reward functions to formulate the sparse rewards to train our navigation policies: Goal distance reward r_{dist} , Goal heading reward r_{head} , and Elevation reward r_{elev} to formulate the sparse rewards to train our navigation policies. Hence,

$$r_{dist} = \frac{\beta}{2} \mathcal{N}\left(\frac{d_{goal}}{2}, \sigma^2\right) + \beta \mathcal{N}(0, \sigma^2), \quad (8)$$

$$r_{head} = \mathbb{I}_{\{|\alpha_{goal}| \leq \pi/3\}}, \quad (9)$$

where, \mathcal{N} denotes Gaussian distribution with variance σ and β is the amplitude parameter. We set the variance $\sigma = 0.2$ to ensure that the r_{dist} only includes two narrow reward peaks near the goal and half-way from the goal. Similarly, r_{elev} is defined as $r_{elev} = \mathbb{I}_{\{|\phi| \geq \pi/6\}} \cup \mathbb{I}_{\{|\theta| \geq \pi/6\}}$. We observe that our reward definitions are significantly sparse compared to the traditional dense rewards used in the literature [31].

(a) Even terrain navigation: The robot is placed in an obstacle-free even terrain environment and random goals in the range of 10-15 meters away from the starting position are given at each episode. The state space is $s = [d_{goal}, \alpha_{goal}]$ and the overall reward formulation $r_{even} = r_{goal} + r_{head}$.

(b) Uneven terrain navigation: The robot is placed in an obstacle-free, highly uneven terrain environment. The state space is $s = [d_{goal}, \alpha_{goal}, \phi, \theta]$. The objective is to navigate the robot to a goal location along relatively even terrain regions to avoid possible robot flip-overs. The overall reward formulation $r_{uneven} = r_{goal} + r_{head} + r_{elev}$.

(c) Real-world Experiments: The real and simulated testing were conducted in different outdoor scenarios. Particularly, the real-world environments are reasonably different in terms of terrain structure (i.e. elevation gradient) and surface properties (i.e grass and tiny gravel regions with

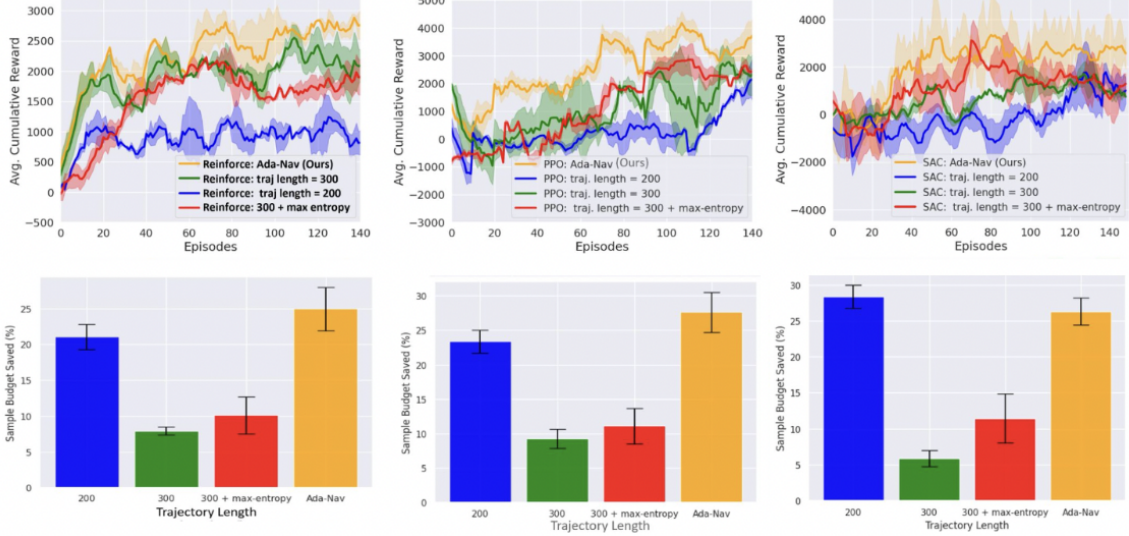


Fig. 4: [TOP] Learning curves during training and [BOTTOM] sample complexity savings during navigation tasks for the even terrain shown on the left of Figure 3. Comparison of [LEFT] REINFORCE, [MIDDLE] PPO, and [RIGHT] SAC, with constant and adaptive trajectory lengths. For each algorithm, Ada-NAV converges to a higher cumulative reward while expending less of the total budget of $\sim 4.5e4$ samples. We ran 8 to 10 independent replications for each of the 12 experiments. Although fixed trajectory length 200 performs comparably to Ada-NAV in terms of sample complexity, it achieves lower reward in all cases.

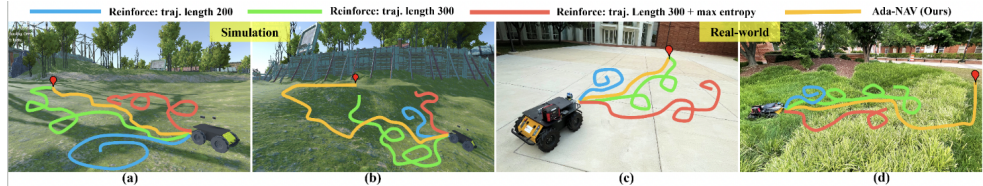


Fig. 5: Sample navigation trajectories generated in simulated and real-world environments by policies trained using Ada-NAV vs. fixed trajectory lengths at a fixed sample budget of $\sim 4.5e4$. We observe that the fixed trajectory length policies often fail at test time due to inefficient use of the available sample budget during training. In contrast, Ada-NAV policies successfully complete the navigation tasks after training with the same sample budget. Further, the experiments with a real Clearpath Husky robot validate that our method can be transferred onto real robotic systems without significant performance degradation. The drawn trajectories are sample representations of the robot's odometry data collected during each task.

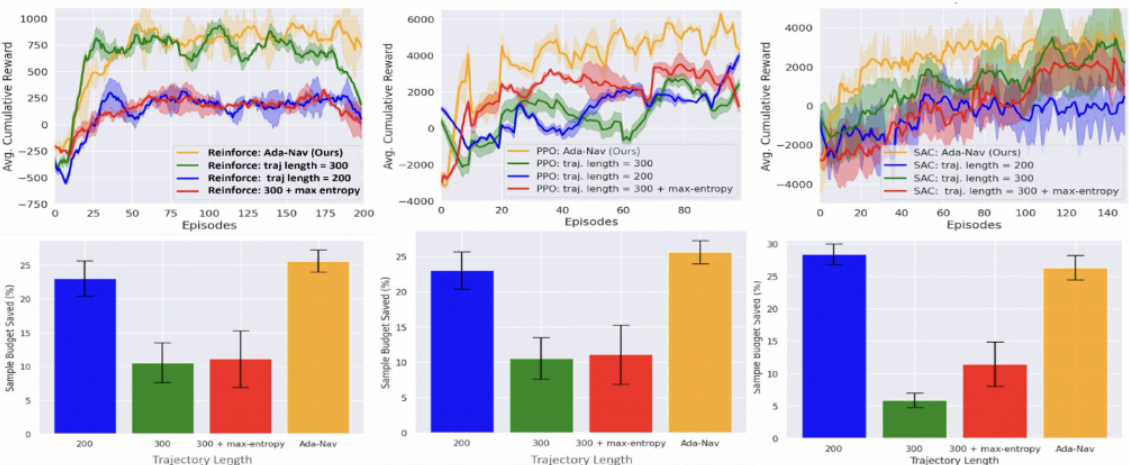


Fig. 6: [TOP] Learning curves during training and [BOTTOM] sample complexity savings during navigation tasks for the uneven terrain shown on the right of Figure 3. Comparison of [LEFT] REINFORCE, [MIDDLE] PPO, and [RIGHT] SAC, with constant and adaptive trajectory lengths. For each algorithm, Ada-NAV converges to a higher cumulative reward while expending less of the total budget of $\sim 4.5e4$ samples. We ran 8 to 10 independent replications for each of the 12 experiments. Although fixed trajectory length 200 performs comparably to Ada-NAV in terms of sample complexity, it achieves lower reward in all cases.

different levels of friction) which are not included or modeled in the simulator (e.g. elevation gain in the simulator is up to $\sim 4m$, however, we restricted it to $\sim 1.5m$ elevation gain in the real world for robot’s safety). Our Clearpath Husky robot is equipped with a VLP16 LiDAR and a laptop with an Intel i9 CPU and an Nvidia RTX 2080 GPU.

Terrain	Algorithm	SR (%) \uparrow	PL (# m) \downarrow	EC (m) \downarrow
Even	Reinforce: traj. length = 300 + max entropy	58	22.47	-
	Reinforce: traj. length = 200	32	25.58	-
	Reinforce: traj. length = 300	65	18.75	-
	Ada-NAV(Ours)	84	11.62	-
Uneven	Ego-graph [48]	54	20.36	2.189
	Reinforce: traj. length = 300 + max entropy	28	41.32	3.163
	Reinforce: traj. length = 200	8	9.25	3.116
	Reinforce: traj. length = 300	31	32.44	2.236
	Ada-NAV(Ours)	72	16.28	1.985

TABLE I: Navigation performance of the policies trained for even and uneven terrain navigation tasks at a fixed sample budget. SR denotes success rate, PL denotes average path length, and EC denotes elevation cost. Each method is tested for 100 trials in the outdoor simulator and the average values are reported in the table. Test environments are different from training environments.

A. Evaluation Metrics

We use the following metrics to evaluate the quality of the navigation paths generated with a fixed sample budget:

- **Success rate:** The percentage of successful goal-reaching attempts without robot flip-overs (especially in uneven terrain) out of the total number of trials.
- **Average path length:** The average length of the path taken to reach a goal located 10 meters away from the robot’s starting position.
- **Elevation cost:** The total elevation gradient experienced by the robot during a trial (i.e., if z_r is the vector that includes the gradient of the vertical motions of the robot along a path, the elevation cost is given by $\|\nabla z_r\|$).

B. Results and Discussions

Policy Learning: We observe in Figure 4 and 6 that, for the outdoor robot simulator, Ada-NAV achieves similar or better reward returns with significantly fewer samples under both the navigation settings compared to the fixed and random trajectory lengths. Significantly, despite providing comparable returns to Ada-NAV, the sample efficiency of the constant and large trajectory lengths is significantly lower (see the bar plots in Fig. 4 and 6). Please see the Appendix for similar results in 2D gridworld environments with actor-critic algorithm [49].

Navigation Performance: We compare our method’s navigation performance qualitatively in Fig. 5 and quantitatively in Table I. To highlight the importance of sample efficiency during training, we use policies trained for a fixed sample budget to perform navigation tasks in even and uneven simulated terrains. We observe that, except Ada-NAV, the policies cannot consistently complete the navigation tasks, resulting in significantly lower success rates. Even successful trials of these policies lead to significantly longer paths with several loops instead of heading toward the goal. In contrast, Ada-NAV results in relatively straight and consistent paths toward the goals. We further observe that uneven terrain navigation is a comparatively challenging task even for

traditional methods such as Ego-graph [48]. Hence, the success rates are relatively low due to the robot flip-overs that occurred during trials. However, we observe that Ada-NAV leads to higher success rates even compared to baseline methods such as ego-graph. We further observe that Ada-NAV results in comparatively lower elevation cost indicating that the generated paths are smoother in uneven terrain conditions. Finally, we deploy the policies trained with the outdoor simulator in the real world using a Clearpath Husky robot. We observe that our Ada-NAV even and uneven terrain navigation policies can be transferred to the real world without significant performance degradation in terms of success rate, path length, and elevation cost while other policies demonstrate inconsistent navigation performance similar to the simulations.

V. CONCLUSIONS, LIMITATIONS, AND FUTURE WORKS

In this work, we propose an adaptive trajectory scheme, called Ada-NAV, which encourages exploration and induces training sample efficiency for goal-reaching navigation in the sparse reward setting with RL-based methods. We do so by empirically establishing a positive correlation between a policy’s entropy and the spectral gap of its induced Markov Chain. We show, through experiments in navigation tasks, that Ada-NAV induces more sample-efficient training than both fixed and random trajectory length schemes without the need for tuning. In experiments on real robots, Ada-NAV-trained policies generally achieve better success rates and shorter path lengths than policies trained using constant and random trajectory lengths for the same sample budget.

An important limitation of the present work is the restricted scope of our experimental investigation of the connection between policy entropy and the induced spectral gap. We considered only simple gridworld environments for the purposes of this paper, yet this important connection merits further investigation and validation on more sophisticated challenges, such as the MuJoCo suite of RL problems [50]. During real-world experiments, we observe that all the navigation policies often lead to high motor vibrations due to dynamically infeasible velocities provided as the action. Hence, further investigation is required to generate dynamically feasible and smooth actions for a better sim-to-real transfer.

VI. ACKNOWLEDGEMENTS

This research was supported by Army Cooperative Agreement W911NF2120076 and ARO Grant ARO Grant, W911NF2310352

Disclaimer: This paper was prepared for informational purposes in part by the Artificial Intelligence Research group of JPMorgan Chase & Co and its affiliates (“JP Morgan”), and is not a product of the Research Department of JP Morgan. JP Morgan makes no representation and warranty whatsoever and disclaims all liability, for the completeness, accuracy or reliability of the information contained herein. This document is not intended as investment research or investment advice, or a recommendation, offer or solicitation for the purchase or sale of any security, financial instrument, financial product or service, or to be used in any way for evaluating the merits of participating in any transaction, and

shall not constitute a solicitation under any jurisdiction or to any person, if such solicitation under such jurisdiction or to such person would be unlawful.

REFERENCES

- [1] M. Abdeh, F. Abut, and F. Akay, “Autonomous navigation in search and rescue simulated environment using deep reinforcement learning,” *Balkan Journal of Electrical and Computer Engineering*, vol. 9, no. 2, pp. 92 – 98, 2021.
- [2] R. R. Murphy, *Disaster robotics*. MIT press, 2014.
- [3] K. Schilling, “Autonomous navigation of rovers for planetary exploration,” *IFAC Proceedings Volumes*, vol. 31, no. 21, pp. 83–87, 1998, 14th IFAC Symposium on Automatic Control in Aerospace 1998, Seoul, Korea, 24–28 August 1998.
- [4] J. Canny, *The complexity of robot motion planning*. MIT press, 1988.
- [5] D. Manocha, *Algebraic and numeric techniques in modeling and robotics*. University of California, Berkeley, 1992.
- [6] S. LaValle, “Planning algorithms,” *Cambridge University Press google schola*, vol. 2, pp. 3671–3678, 2006.
- [7] R. S. Sutton and A. G. Barto, *Reinforcement learning: An introduction*. MIT press, 2018.
- [8] K. Zhu and T. Zhang, “Deep reinforcement learning based mobile robot navigation: A review,” *Tsinghua Science and Technology*, vol. 26, no. 5, pp. 674–691, 2021.
- [9] A. Banino, C. Barry, B. Uria, C. Blundell, T. Lillicrap, P. Mirowski, A. Pritzel, M. J. Chadwick, T. Degris, J. Modyai, *et al.*, “Vector-based navigation using grid-like representations in artificial agents,” *Nature*, vol. 557, no. 7705, pp. 429–433, 2018.
- [10] K. Zhu and T. Zhang, “Deep reinforcement learning based mobile robot navigation: A review,” *Tsinghua Science and Technology*, vol. 26, no. 5, pp. 674–691, 2021.
- [11] D. Pathak, P. Agrawal, A. A. Efros, and T. Darrell, “Curiosity-driven exploration by self-supervised prediction,” in *International conference on machine learning*. PMLR, 2017, pp. 2778–2787.
- [12] S. Chakraborty, A. S. Bedi, A. Koppel, P. Tokek, and D. Manocha, “Dealing with sparse rewards in continuous control robotics via heavy-tailed policies,” *arXiv*, 2022.
- [13] D. Rengarajan, G. Vaidya, A. Sarvesh, D. Kalathil, and S. Shakkottai, “Reinforcement learning with sparse rewards using guidance from offline demonstration,” in *International Conference on Learning Representations*, 2021.
- [14] J. Hare, “Dealing with sparse rewards in reinforcement learning,” *arXiv preprint arXiv:1910.09281*, 2019.
- [15] C. Wang, J. Wang, J. Wang, and X. Zhang, “Deep-reinforcement-learning-based autonomous uav navigation with sparse rewards,” *IEEE Internet of Things Journal*, 02 2020.
- [16] A. S. Bedi, A. Parayil, J. Zhang, M. Wang, and A. Koppel, “On the sample complexity and metastability of heavy-tailed policy search in continuous control,” *arXiv preprint arXiv:2106.08414*, 2021.
- [17] K. Weerakoon, S. Chakraborty, N. Karapetyan, A. J. Sathyamoorthy, A. Bedi, and D. Manocha, “HTRON: Efficient outdoor navigation with sparse rewards via heavy tailed adaptive reinforce algorithm,” in *6th Annual Conference on Robot Learning*, 2022.
- [18] H.-T. L. Chiang, A. Faust, M. Fiser, and A. Francis, “Learning navigation behaviors end-to-end with autorl,” *IEEE Robotics and Automation Letters*, vol. 4, no. 2, pp. 2007–2014, 2019.
- [19] M. Vecerik, T. Hester, J. Scholz, F. Wang, O. Pietquin, B. Piot, N. Heess, T. Rothörl, T. Lampe, and M. Riedmiller, “Leveraging demonstrations for deep reinforcement learning on robotics problems with sparse rewards,” *arXiv preprint arXiv:1707.08817*, 2017.
- [20] H. Karnan, G. Warnell, X. Xiao, and P. Stone, “Voila: Visual-observation-only imitation learning for autonomous navigation,” *arXiv preprint arXiv:2105.09371*, 2021.
- [21] R. Houthooft, X. Chen, Y. Duan, J. Schulman, F. De Turck, and P. Abbeel, “Vime: Variational information maximizing exploration,” *Advances in neural information processing systems*, vol. 29, 2016.
- [22] A. Konar, B. H. Baghi, and G. Dudek, “Learning goal conditioned socially compliant navigation from demonstration using risk-based features,” *IEEE Robotics and Automation Letters*, vol. 6, no. 2, pp. 651–658, 2021.
- [23] G. Z. Holland, E. Talvitie, and M. Bowling, “The effect of planning shape on dyna-style planning in high-dimensional state spaces,” *CoRR*, vol. abs/1806.01825, 2018.
- [24] W. A. Suttle, A. Bedi, B. Patel, B. M. Sadler, A. Koppel, and D. Manocha, “Beyond exponentially fast mixing in average-reward reinforcement learning via multi-level monte carlo actor-critic,” in *International Conference on Machine Learning*. PMLR, 2023, pp. 33 240–33 267.
- [25] D. J. Hsu, A. Kontorovich, and C. Szepesvári, “Mixing time estimation in reversible markov chains from a single sample path,” *CoRR*, vol. abs/1506.02903, 2015.
- [26] G. Wolfer, “Mixing time estimation in ergodic markov chains from a single trajectory with contraction methods,” in *Proceedings of the 31st International Conference on Algorithmic Learning Theory*, ser. Proceedings of Machine Learning Research, A. Kontorovich and G. Neu, Eds., vol. 117. PMLR, 08 Feb–11 Feb 2020, pp. 890–905.
- [27] R. J. Williams, “Simple statistical gradient-following algorithms for connectionist reinforcement learning,” *Machine learning*, vol. 8, no. 3, pp. 229–256, 1992.
- [28] J. Schulman, F. Wolski, P. Dhariwal, A. Radford, and O. Klimov, “Proximal policy optimization algorithms,” *arXiv preprint arXiv:1707.06347*, 2017.
- [29] T. Haarnoja, A. Zhou, P. Abbeel, and S. Levine, “Soft actor-critic: Off-policy maximum entropy deep reinforcement learning with a stochastic actor,” in *International conference on machine learning*. PMLR, 2018, pp. 1861–1870.
- [30] X. Xiao, B. Liu, G. Warnell, and P. Stone, “Motion planning and control for mobile robot navigation using machine learning: a survey,” *Autonomous Robots*, pp. 1–29, 2022.
- [31] K. Weerakoon, A. J. Sathyamoorthy, U. Patel, and D. Manocha, “Terp: Reliable planning in uneven outdoor environments using deep reinforcement learning,” in *2022 International Conference on Robotics and Automation (ICRA)*, 2022, pp. 9447–9453.
- [32] K. Zhang, F. Nirouei, M. Ficocelli, and G. Nejat, “Robot navigation of environments with unknown rough terrain using deep reinforcement learning,” in *2018 IEEE International Symposium on Safety, Security, and Rescue Robotics (SSRR)*. IEEE, 2018, pp. 1–7.
- [33] S. Josef and A. Degani, “Deep reinforcement learning for safe local planning of a ground vehicle in unknown rough terrain,” *IEEE Robotics and Automation Letters*, vol. 5, no. 4, pp. 6748–6755, 2020.
- [34] G. Brunner, O. Richter, Y. Wang, and R. Wattenhofer, “Teaching a machine to read maps with deep reinforcement learning,” in *Proceedings of the AAAI Conference on Artificial Intelligence*, vol. 32, no. 1, 2018.
- [35] A. Staroverov, D. A. Yudin, I. Belkin, V. Adeshkin, Y. K. Solomentsev, and A. I. Panov, “Real-time object navigation with deep neural networks and hierarchical reinforcement learning,” *IEEE Access*, vol. 8, pp. 195 608–195 621, 2020.
- [36] J. Costa de Jesus, V. Kich, A. Kolling, R. Grando, M. Cuadros, and D. F. Gamarra, “Soft actor-critic for navigation of mobile robots,” *Journal of Intelligent & Robotic Systems*, vol. 102, 06 2021.
- [37] A. Zai and B. Brown, *Deep reinforcement learning in action*. Manning Publications, 2020.
- [38] N. Botteghi, B. Sirmacek, K. A. Mustafa, M. Poel, and S. Stramigioli, “On reward shaping for mobile robot navigation: A reinforcement learning and slam based approach,” *arXiv preprint arXiv:2002.04109*, 2020.
- [39] A. Nair, B. McGrew, M. Andrychowicz, W. Zaremba, and P. Abbeel, “Overcoming exploration in reinforcement learning with demonstrations,” in *2018 IEEE international conference on robotics and automation (ICRA)*. IEEE, 2018, pp. 6292–6299.
- [40] C. Wang, G. Warnell, and P. Stone, “D-shape: Demonstration-shaped reinforcement learning via goal conditioning,” 2023.
- [41] S. Ao, T. Zhou, G. Long, Q. Lu, L. Zhu, and J. Jiang, “Copilot: Collaborative planning and reinforcement learning on sub-task curriculum,” in *Advances in Neural Information Processing Systems*, M. Ranzato, A. Beygelzimer, Y. Dauphin, P. Liang, and J. W. Vaughan, Eds., vol. 34. Curran Associates, Inc., 2021, pp. 10 444–10 456.
- [42] A. S. Bedi, S. Chakraborty, A. Parayil, B. M. Sadler, P. Tokek, and A. Koppel, “On the hidden biases of policy mirror ascent in continuous action spaces,” *CoRR*, vol. abs/2201.12332, 2022.
- [43] R. S. Sutton, D. McAllester, S. Singh, and Y. Mansour, “Policy gradient methods for reinforcement learning with function approximation,” *Advances in neural information processing systems*, vol. 12, 1999.
- [44] A. S. Bedi, A. Parayil, J. Zhang, M. Wang, and A. Koppel, “On the sample complexity and metastability of heavy-tailed policy search in continuous control,” *arXiv preprint arXiv:2106.08414*, 2021.
- [45] R. Dorfman and K. Y. Levy, “Adapting to mixing time in stochastic optimization with Markovian data,” in *Proceedings of the 39th International Conference on Machine Learning*, ser. Proceedings of Machine Learning Research, K. Chaudhuri, S. Jegelka, L. Song, C. Szepesvari, G. Niu, and S. Sabato, Eds., vol. 162. PMLR, 17–23 Jul 2022, pp. 5429–5446.
- [46] D. A. Levin and Y. Peres, *Markov chains and mixing times*. American Mathematical Soc., 2017, vol. 107.
- [47] C. E. Shannon, “A mathematical theory of communication,” *The Bell System Technical Journal*, vol. 27, pp. 379–423, 1948.

- [48] S. Josef and A. Degani, “Deep reinforcement learning for safe local planning of a ground vehicle in unknown rough terrain,” *IEEE Robotics and Automation Letters*, vol. 5, no. 4, pp. 6748–6755, 2020.
- [49] V. Konda and J. Tsitsiklis, “Actor-critic algorithms,” in *Advances in Neural Information Processing Systems*, S. Solla, T. Leen, and K. Müller, Eds., vol. 12. MIT Press, 1999.
- [50] E. Todorov, T. Erez, and Y. Tassa, “Mujoco: A physics engine for model-based control,” in *2012 IEEE/RSJ International Conference on Intelligent Robots and Systems*. IEEE, 2012, pp. 5026–5033.

VII. APPENDIX

A. Experimental Setup Details

Here are the full descriptions of navigation experiments. The first one details the Clearpath Husky simulation experiments in even and uneven terrain shown in the main body. The second one explains the real robotic experiments also shown in the main body. The third set of experiments shows the benefits of Ada-NAV with Actor-Critic (AC) in 2D gridworld:

- 1) **Even and Uneven Terrain Navigation in Robotic Simulations:** We use a Unity-based outdoor simulator with a Clearpath Husky robot model to train policies for two navigation tasks: 1. Goal Reaching, 2. Uneven terrain navigation using the Reinforce algorithms. The Unity simulator includes diverse terrains and elevations for training and testing. We restrict ourselves to a $100m \times 100m$ region during training. We used identical policy distribution parameters and neural network architectures with all four algorithms during training and evaluation. The policies are implemented using Pytorch in to train in the simulator equipped with a Clearpath Husky robot model, and a ROS Melodic platform. The training and simulations are executed on a workstation with an Intel Xeon 3.6 GHz CPU and an Nvidia Titan GPU. Our agent is a differential drive robot with a two-dimensional continuous action space $a = (v, \omega)$ (i.e. linear and angular velocities). The state space varies for the two navigation tasks and is obtained in real time from the simulated robot's odometry and IMU sensors. The state inputs used in the two scenarios are, leftmargin=*

- $d_{goal} \in [0, 1]$ - Normalized distance (w.r.t the initial straight line distance) between the robot and its goal;
- $\alpha_{goal} \in [0, \pi]$ - Angle between the robot's heading direction and the goal;
- $(\phi, \theta) \in [0, \pi]$ - Roll and pitch angle of the robot respectively;

Inspired by [17], we define three reward functions: Goal distance reward r_{dist} , Goal heading reward r_{head} , and Elevation reward r_{elev} to formulate the sparse rewards to train our navigation policies. Hence,

$$r_{dist} = \frac{\beta}{2} \mathcal{N}\left(\frac{d_{goal}}{2}, \sigma^2\right) + \beta \mathcal{N}(0, \sigma^2) \quad \text{and, } r_{head} = \mathbb{1}_{\{|\alpha_{goal}| \leq \pi/3\}} \quad (10)$$

where, \mathcal{N} denotes Gaussian distribution with variance σ and β is the amplitude parameter. We set the variance $\sigma = 0.2$ to ensure that the r_{dist} only includes two narrow reward peaks near the goal and half-way from the goal. Similarly, r_{elev} is defines as,

$$r_{elev} = \mathbb{1}_{\{|\phi| \geq \pi/6\}} \cup \mathbb{1}_{\{|\theta| \geq \pi/6\}}. \quad (11)$$

We observe that our reward definitions are significantly sparse compared to the traditional dense rewards used in literature [31].

- 2) **(a) Even terrain navigation:** The robot is placed in an obstacle-free even terrain environment and random goals in the range of 10-15 meters away from the starting position is given at each episode. The state space is $s = [d_{goal}, \alpha_{goal}]$ and the overall reward formulation $r_{even} = r_{goal} + r_{head}$.
- 2) **(b) Uneven terrain navigation:** The robot is placed in an obstacle-free, highly uneven terrain environment. The state space is $s = [d_{goal}, \alpha_{goal}, \phi, \theta]$. The objective is to navigate the robot to a goal location along relatively even terrain regions to avoid possible robot flip overs. The overall reward formulation $r_{uneven} = r_{goal} + r_{head} + r_{elev}$.
- 2) **Real-world Experiments:** The real and simulated testing were conducted in different outdoor scenarios. Particularly, the real-world environments are reasonably different in terms of terrain structure(i.e. elevation gradient) and surface properties(i.e grass and tiny gravel regions with different levels of friction) which are not included or modeled in the simulator (e.g. elevation gain in the simulator is up to $\sim 4m$, however, we restricted it to $\sim 1.5m$ elevation gain in the real world for robot's safety). Our Clearpath Husky robot is equipped with a VLP16 LiDAR and a laptop with an Intel i9 CPU and an Nvidia RTX 2080 GPU.
- 3) **Increasing Obstacles in 2D gridworld:** Agent starts at the top left of a 25-by-25 grid and navigates to the bottom right. The agent can move up, down, left, right, or stay. It gains a reward of +1 for reaching the goal and +0 otherwise. We have three different gridworlds: one with no obstacles and two with walls. If the agent takes an action that would cause it to collide with a wall, it will just stay in its current location. We use Actor-Critic method and compare against fixed trajectory length and randomly-sampled trajectory length (MAC) [24]. Because of the state and action space are both discrete, our implementation involves using a linear approximator for each state-action pair and then a softmax operation for the actor and another linear approximator for each state for the critic.

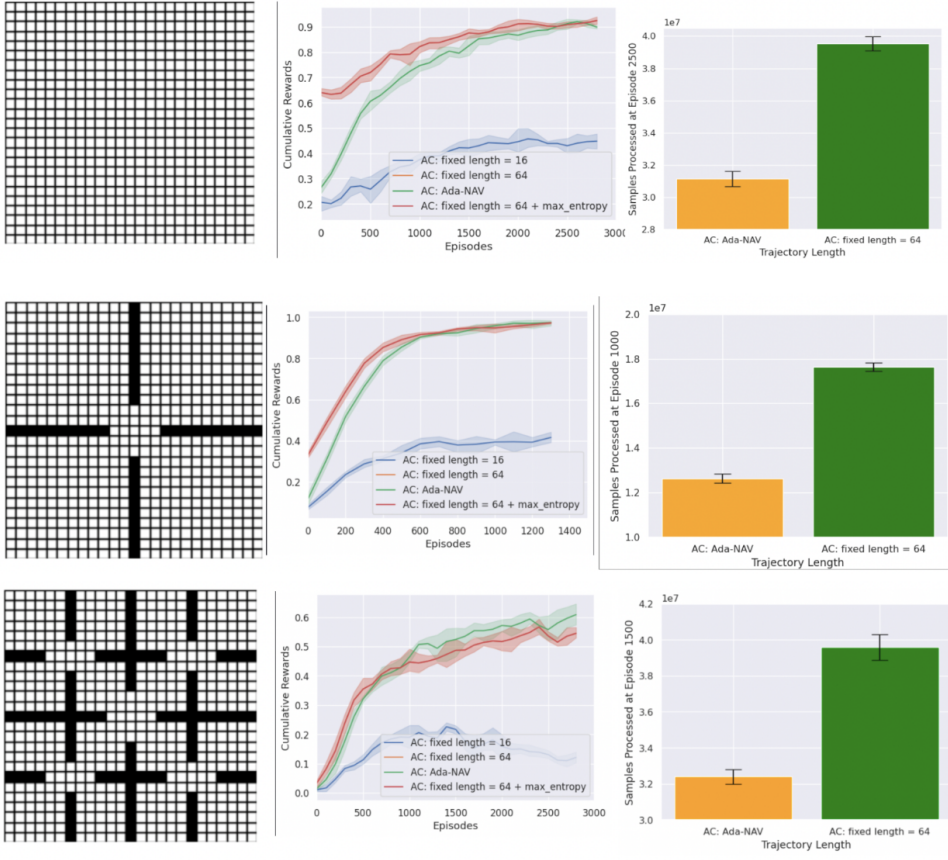


Fig. 7: 25-by-25 gridworld environments with Actor-Critic with constant and adaptive trajectory and constant trajectory with max-entropy regularization for learning navigation to bottom right. [LEFT] Visualization of the grid environment where white represents open space and black represents walls. [MIDDLE] The mean cumulative rewards over 2500 episodes. [RIGHT] The number of samples processed between adaptive length and constant length 64.

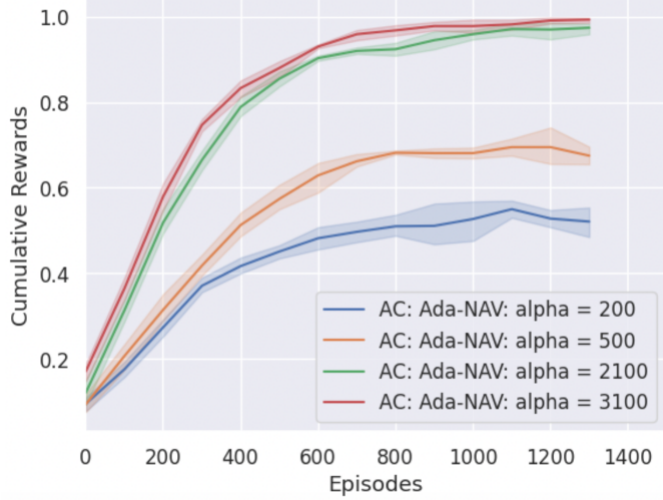


Fig. 8: We train Ada-NAV models in the 4 wall environment with changing values of α for five trials each. The t_i for all models is 16. We see that as α decreases, the RL agents converge to suboptimal rewards.

To show that other monotonic transformations between policy entropy and trajectory length can be used, we trained another AC model for five trials with Ada-NAV trajectory selection scheme using an exponential mapping:

$$t_c = f(H_c) = \text{round}(t_i e^{\alpha(\frac{H_c}{H_i} - 1)}) \quad (12)$$

Figure 9 shows the training with exponential transformation compared against linear transformation given in Eq 7 and fixed trajectory lengths. We see that the exponential transformation is the most sample efficient.

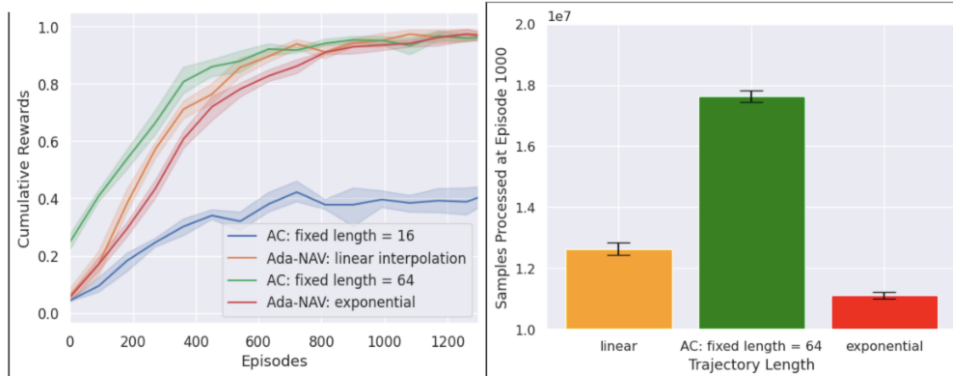


Fig. 9: Training plot in the 4 walls environments with AC. We train two models with Ada-NAV selection scheme: one with linear transformation given in Eq 7 and one with exponential give in Eq 12

TABLE II: This table compares the hyperparameters and performance between the four experiments, each run for five trials

Environment	Model	Trajectory Method	t_d	Trajectory Change	Learning Rate	No. of Iterations Per Episode
2D Gridworld						
No Obstacles	AC	Fixed = 16			0.01	500
No Obstacles	AC	Fixed = 64			0.01	500
No Obstacles	AC	Ada-NAV			0.01	500
No Obstacles	AC + max-entropy	Fixed = 64	1100	16 → 56	0.01	500
4 Walls	AC	Fixed = 16			0.01	500
4 Walls	AC	Fixed = 64			0.01	500
4 Walls	AC	Ada-NAV			0.01	500
4 Walls	AC + max-entropy	Fixed = 64	2100	16 → 61	0.01	500
16 Walls	AC	Fixed = 16			0.01	500
16 Walls	AC	Fixed = 64			0.01	500
16 Walls	AC	Ada-NAV			0.01	500
16 Walls	AC + max-entropy	Fixed = 64	2100	16 → 69	0.01	500
Robot Simulations						
Even Terrain	REINFORCE	Fixed = 200			0.0001	400
	REINFORCE	Fixed = 300			0.0001	400
	REINFORCE	Ada-NAV			0.0001	400
	REINFORCE	Fixed = 300 + max entropy	3200	180 → 300	0.0001	400
Uneven Terrain	REINFORCE	Fixed = 200			0.0001	400
	REINFORCE	Fixed = 300			0.0001	400
	REINFORCE	Ada-NAV			0.0001	400
	REINFORCE	Fixed = 300 + max entropy	3200	200 → 300	0.0001	400